
A neuromorphic boost to RNNs using low pass filters

Manu V Nair

Institute of Neuroinformatics | Synthara AG
University of Zurich-ETH Zurich
mnair@ini.uzh.ch | manu@synthara.ch

Giacomo Indiveri

Institute of Neuroinformatics
University of Zurich-ETH Zurich
giacomo@uzh.ch

Abstract

The increasing difficulty with Moore’s law scaling and the remarkable success of machine learning have triggered a renaissance in the study of low-latency, energy-efficient accelerators for machine learning applications. In particular, spiking neural networks (SNNs) and their neuromorphic hardware implementations have started to receive substantial attention from academia and industry. However, SNNs perform relatively poorly compared to their rate-based counterparts, in terms of accuracy in pattern recognition tasks. In this paper, we present a low pass recurrent neural network (lpRNN) cell that can be trained using backpropagation and implemented on neuromorphic SNN devices. The ability to implement our model on neuromorphic hardware enables the construction of compact devices that can perform always-on processing in ultra-low power edge computing applications. We further argue that the low pass filter is a temporal regularizer and highlight its advantage in a Long Short-Term Memory (LSTM) cell. We show that low pass RNNs are able to learn and generalize better than their unfiltered variants on two long memory synthetic tasks, a character-level text modeling task, and a neuromorphic spoken command detection system.

1 Introduction

Exponential growth in computational power and efficiency in graphical processing units (GPUs), and more generally, on von Neumann platforms [1] (such as x86 [2] and ARM [3] platforms), have played a key role in the development of neural networks and their training algorithms. However, it has also led to higher design complexity and an increasingly difficult to keep up with Moore’s law today [4, 5]. Recent years have also seen the movement of computation from data-centres to compact, distributed, and portable embedded systems. These factors have created an increasing demand for energy efficient AI-capable devices, leading to the development of dedicated and optimized von Neumann-style AI accelerators [6–8] and a renewed interest in alternative brain-inspired, event-based neuromorphic computing platforms [9–14].

An important difference between artificial neural networks (ANN) deployed on GPUs and on (most) neuromorphic platforms is the use of spikes or train of pulses to represent signals. Such networks are called spiking neural networks (SNN). We distinguish between ANNs and SNNs in this paper as follows: By ANNs, we refer to popular deep learning neural networks (such as LSTMs) that are trained using the back-propagation algorithm (backprop). SNNs refers to neural networks that use spike trains to communicate between the different nodes of the network and have much richer internal dynamics than their ANN counterparts. However, the dynamical nature of SNNs makes them very difficult to train using conventional optimization tools like backprop. Neuromorphic systems use SNNs with the goal to mimic biology and/or achieve low-power computation. SNNs are interesting because they use an array of distributed computing nodes that use in-memory and asynchronous computation techniques making them very power efficient [15–17]. We propose an ANN low pass

RNN (lpRNN) cell which can be trained using backprop, and have the added advantage that they can be mapped to an SNN suitable for neuromorphic platforms.

A common problem that SNNs have is related to the way they encode signals. Researchers have suggested various techniques to do this [18–21], that typically use rate [18] or time-coded [19] spike-generation schemes. Achieving high data-resolution with rate coding requires a large number of spikes which is not energy-efficient [22]. On the other hand, codecs for time-coding are complex, especially on hardware that is subject to mismatch and noise. The solution proposed in this paper is the use of the adaptive integrate and fire neuron model, which is interpreted as an asynchronous $\Delta\Sigma$ circuit [20]. We note that low pass filters acts as a temporal regularizer and extend the LSTM cell to incorporate this feature. The resulting lpLSTM cell demonstrates a more stable convergence behaviour than the original LSTM cell. We illustrate its effect on two tasks. We train the RNN cells using a curriculum learning protocol [23] and find that they are able to retain information for much longer than reported in the literature so far. Finally, we demonstrate the use of the lpRNN cell in a neuromorphic system on a limited vocabulary spoken command detection task using the Google commands dataset [24].

2 Modeling a spiking neuron

Coding mechanism A neuron in deep learning has one primary function - the non-linear transformation of its input. However, a biological neuron and its neuromorphic counterpart have the added job of encoding information in spike trains. The most popular model for this encoding mechanism is rate coding, where the neuron fires at a rate proportional to the incoming signal. This mechanism is not efficient for transmitting high-resolution data. For example, to transmit a signal at 8-bit resolution, it will require $O(256)$ spikes for each sample. An improvement to this coding mechanism is the adaptive integrate and fire model [25], which can be interpreted as an asynchronous delta-sigma ($\Delta\Sigma$) loop [26, 20, 22]. The $\Delta\Sigma$ mechanism is more efficient in its use of spike trains [22]. Other time coding schemes have been proposed in literature [19, 27]. However, the advantage of the $\Delta\Sigma$ interpretation is that leads to highly power-efficient circuit implementations [22]. It allows us to treat the neuron state as an analogue variable and ignoring the specific timing details of the encoding spike trains [22]. This is very useful because state-dependence, noise and device mismatch cause each neuron to generate spikes at different times for the same input. The $\Delta\Sigma$ loop ensures that they all represent the same signal with the same accuracy [22]. This enables the network designer to only look at the internal state of the neuron when optimizing the network weights for an SNN. *This abstraction is a key enabler for this paper as simulating and training mismatch-prone SNNs is computationally much more expensive than ANNs.*

Biological neural networks are low pass filtering Activation functions used in all neural networks sum incoming signals weighted by the synaptic weights and apply a non-linearity. However, ANNs assume that when the input changes, the internal state of the neuron or dendrites can also change immediately to reflect the new input. This behaviour ignores the fact that biological neuronal channels are low-pass filters [27]. Modelling the inertial or low-pass filtering property is essential to implement and study recurrent neural networks in any neuromorphic system as the transitional dynamics deviate completely in its absence. We argue that not only is this modelling essential, it is also a useful constraint to impose on RNNs.

3 The low pass recurrent neural network

We incorporate a discrete-time low pass filtering term at the output of RNN stage. This results in the low pass RNN (lpRNN) cell that has the following update equation:

$$y_t = \alpha \odot y_{t-1} + (1 - \alpha) \odot \sigma(W_{rec} \cdot y_{t-1} + W_{in} \cdot x_t + b) \quad (1)$$

where, σ , \odot and \cdot denote non-linearity, element-wise Hadamard product and matrix multiplication functions, respectively. The variables α , y_n , x_n , W_{rec} , W_{in} , and b represent the retention ratio vector, input vector, output vector, recurrent connectivity weight matrix, input connectivity weight matrix, and biases, respectively. The subscripts on variable y and x indicate the time step. α is constrained to lie within $[0,1]$. When $\alpha = 0$, equation 1 reduces to that of a simple recurrent neural network (SimpleRNN). The boundary conditions on the retention ratio, $\alpha \in [0, 1]$, can be imposed by passing

it through a sigmoidal non-linearity if it needs to be trained. Keeping α fixed and random simplifies the design of a neuromorphic system by eliminating the need to create tunable time constants in the neuron implementations. There also appears to be no significant advantage in learning it during training if the relu non-linearity is used as it can scale its output to a large value if required. It is also more biologically plausible, as it appears unlikely that neurons or dendrites can accurately set themselves with arbitrary precision. If α is not learnt, the number of trainable parameters in the lpRNN model is the same as a SimpleRNN cell. We train the lpRNN cell using backprop and by use of $\Delta\Sigma$ coding, map it to an equivalent SNN. This mechanism only requires knowledge of the time constants of the spiking neurons to ensure that the lpRNN cell is operating at the same time scale. This mapping mechanism has been demonstrated Figures 1 for an echo-state network (ESN) [28] with 50 hidden units and a linear readout stage trained to distinguish a synthetic input pattern [29]. Note that an ESN formulation is essentially that of an untrained lpRNN cell with spectral radius constraints on the recurrent kernel. The mapped dynamics match with a small normalized mean square error (0.03). The error is mainly concentrated at higher frequency components outside the bandwidth of the SNN.

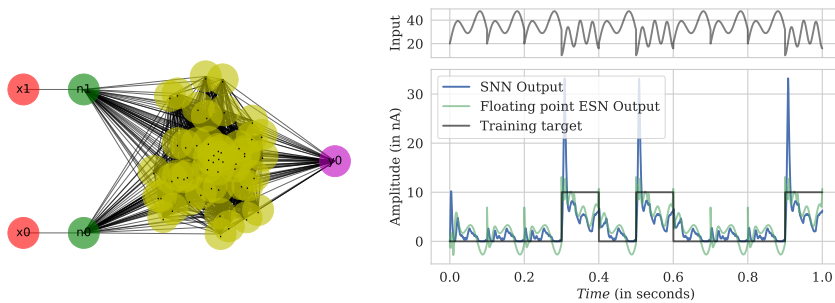


Figure 1: Mapping an lpRNN model to a spiking framework. The read out stage of the ESN (Left) is trained by stochastic gradient descent and mapped to an SNN. The figure on right shows the state of the lpRNN/ESN output and its spiking implementation (SNN Output).

4 The neuromorphic signal chain

The $\Delta\Sigma$ mapping mechanism requires defining suitable time constants for the lpRNN cell being trained by backprop. This can be derived for continuous-time signals from sensors or real-world signals such as an audio input by taking into account the bandwidth of the incoming signals [29]. We illustrate a reference neuromorphic signal chain for processing audio input in Figure 2. The data received from the audio sensor is first filtered by an audio filtering stage such as the cochlea chips [30–32]. These systems typically implement mel-spaced filter banks. A neural network processes the filter outputs and drives an actuator system. A minimal configuration of weights and connectivity required to implement the lpRNN cell in a neuromorphic platform is illustrated in Figure 2. It is a memory array with spiking neurons attached to the periphery of the system. Each memory cell acts as a transconductance stage - it receives voltage spikes and generates a scaled output current. These currents are summed by the Kirchoff's current law and integrated by the neurons. Readers familiar with memory design and computer architecture may identify this as an in-memory computational unit. An in-memory neural network accelerator is energy-efficient, primarily because it eliminates movement of synaptic weights [33, 13] from the memory to a far-away processing module. Instead, the activations of the neurons are transmitted to the other nodes in the network. The computation is no longer memory-bound unlike RNN computation on von Neumann style architecture. Figure 2 implements a single spiking RNN stage (equivalent to an lpRNN), with green and red boxes highlighting the input and recurrent kernels, respectively. The architecture can be modified to implement a fully connected layer by eliminating recurrent connections. Note that an equivalent configuration can be also set up in fully-digital neuromorphic systems such as [9, 10, 12] that do not suffer from noise and mismatch issues, but may consume more area and power.

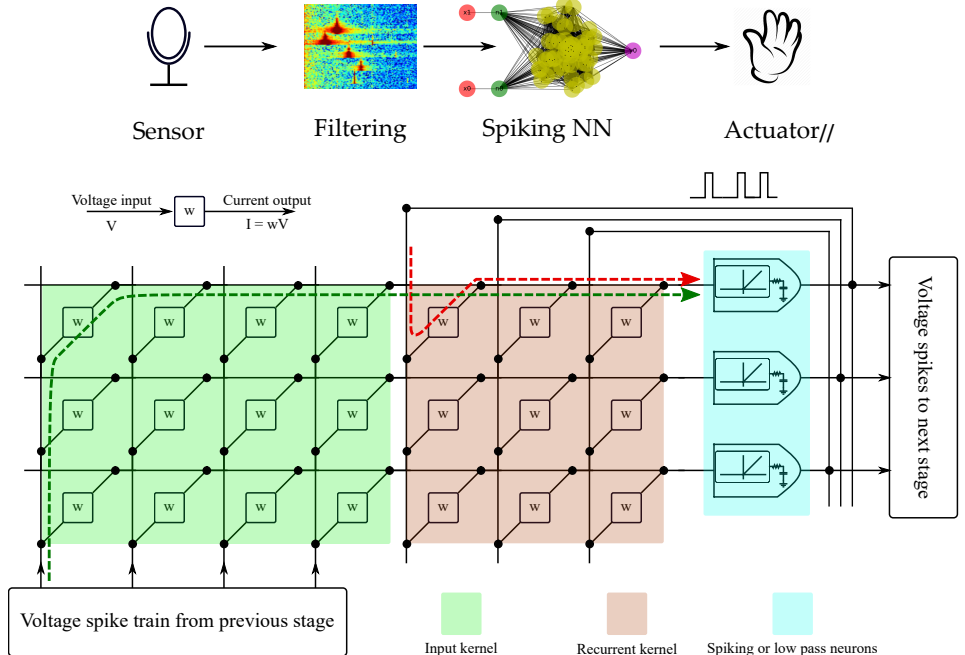


Figure 2: Top: A neuromorphic signal chain. Bottom: Architecture of an SNN accelerator implementing an lpRNN.

5 Comparison to other RNN models

The lpRNN model is closely related to ESNs proposed by Herbert Jaeger [28] where the recurrent layer uses leaky integration units. In ESNs [28], the spectral radius of the initialization values of the recurrent kernel is constrained to approximately 1, which confers an echo-state property to the network. The recurrent or input connectivity weights are not trained during the learning process. Instead, only the read-out linear classifier is trained. In the lpRNN model, the spectral radius of the recurrent kernel is not constrained and all the weight matrices, including the retention ratios if required, are trained. lpRNN also shares similarities with recurrent residual networks proposed by Yiren Wang [34], which are described by the following equations

$$y_t = f(g(y_{t-1})) + \sigma(y_{t-1}, x_t, W) \tag{2}$$

where W denotes input and recurrent kernels, and other symbols have the same meaning as equation 1. In equation 2, g and f are identity and a hyperbolic tangent functions, respectively. A comparison can also be made with the LT-RNN model proposed by Mikael Henaff [35], whose update equations are:

$$h_t = \sigma(W_{in} \cdot x + b) + V \cdot h_{t-1} \tag{3}$$

$$y_t = W \cdot h_t \tag{4}$$

where W and V are 2-D transition matrices that are learned during the training process. In this case, it is possible that the LT-RNN cell reduces to an lpRNN, but is unlikely to occur in practice. Similar analogies can also be made to the IndRNN model [36] and recurrent identity networks [37]. Generally speaking, the main difference between the lpRNN cells and existing RNN models in the literature is the imposition of boundary and train-ability conditions on α , and the applicability of the model for neuromorphic platforms.

6 Memory in an lpRNN

We can analyze the evolution of an lpRNN cell by using an approach similar to the power iteration method, described by Razvan Pascanu [38]. To do this analysis, we approximate the lpRNN update equation as:

$$y_t = \alpha \odot y_{t-1} + (1 - \alpha) \odot (W_{rec} \cdot y_{t-1} + W_{in} \cdot x_t + b) \tag{5}$$

where, for simplicity, we also make the added assumption that all units of the lpRNN layer have the same retention factor, α . The gradient terms during back-propagation through time can now be expressed as a product of several terms that have the form:

$$\frac{\delta y_t}{\delta y_k} = [(1 - \alpha)W_{rec}^T + \alpha]^l \quad (6)$$

where, t and k , are time step indices with $t > k$ and $l = t - k$. If an eigenvalue of the W_{rec}^T matrix is λ , then the corresponding eigenvalue of the matrix $[(1 - \alpha)W_{rec}^T + \alpha]$ can be written as

$$(1 - \alpha)\lambda + \alpha \quad (7)$$

Looking at the eigenvalue of the gradient terms as computed in equation 7, we note that α acts like a **temporal regularizer** on the eigenvalues of the recurrent network. It can also be seen that by scaling α to lie between 0 and 1, the operation of the network shifts between that of purely non-inertial recurrent to a completely inertial network stuck in its initial state, respectively. This insight helps us understand why lpRNNs perform well in long memory tasks.

Hochreiter [39] defined the constant error carousel (CEC) as a central feature of the LSTM networks that allowed it to remember past events. In a crude sense, this corresponds to setting the retention ratio, $\alpha = 1$. Forget gates were subsequently added by Felix A. Gers [40] to the original LSTM structure, that allowed the network to also erase unnecessary events that were potentially trapped in the CEC. This means that the average effective weight of the self-connection in the CEC was made < 1 . A randomly initialized set of α values with a reasonably large number of cells appears to have similar functionality. By setting $\alpha < 1$, the network is guaranteed to lose memory over time, but if some of the α s are close to 1, it may retain the information for a longer time frame. Moreover, the regularization effect of α s also prevents the eigenvalues of the recurrent network from becoming too small, ensuring that memory is never lost immediately. We expect that the lpRNN model has a reduced representational power than gated RNN cells, not simply because it has 4x fewer parameters, but because the lpRNN state is guaranteed to fade with time whereas a gated cell can potentially store a state indefinitely.

Our goal with introducing lpRNN cell was to enable faster and better training of SNNs. However, the analysis performed here indicates that low pass filtering also provides temporal regularization features which can benefit ANN-RNNs such as LSTMs. Therefore, we propose to extend the LSTM formulation by applying a low pass filter at the output (h), and call it an **lpLSTM** cell:

$$\begin{aligned} \text{Forget gate: } f_t &= \text{Sigmoid}(W_f x_t + W_{rec_f} h_{t-1} + b_f) \\ \text{Input gate: } i_t &= \text{Sigmoid}(W_i x_t + W_{rec_i} h_{t-1} + b_i) \\ \text{Output gate: } o_t &= \text{Sigmoid}(W_o x_t + W_{rec_o} h_{t-1} + b_o) \\ \text{State: } c_t &= f_t \odot c_{t-1} + i_t \odot \text{Relu}(W_c x_t + W_{rec_c} h_{t-1} + b_c) \\ \text{Output: } \bar{h}_t &= o_t \odot \text{Relu}(c_t) \\ \text{Filtered Output: } h_t &= \alpha \odot h_{t-1} + (1 - \alpha) \odot \bar{h}_t \end{aligned} \quad (8)$$

where, W_{rec_x} , W_x , b_x indicate the recurrent kernel, input kernel, and bias for the corresponding gate or state. Similar formulations for other RNN cells such as GRU [41], IndRNN [36], Phased-LSTMs [42], Convolutional LSTMs [43], etc can be easily made.

7 Simulations

We illustrate the memory capabilities of the low pass RNN cells using the synthetic addition and copying tasks, that are commonly used for this purpose [39, 44, 45]. In all our tests, we try to keep the number of parameters same for all models. The temporal addition and copying tasks were trained using stochastic gradient descent with a learning rate of 0.01 for lpRNNs and 0.005 for LSTM cells. The normalized gradient was clipped to 1 LSTMs and 1000 for all other models. We highlight the benefits of temporal regularization using the Penn Treebank dataset using the same network architecture and training setting as [46] with lpLSTM swapped in place of the LSTM layers. We also benchmark the lpRNN cell using the Google spoken commands dataset [24]. Adam optimizer [47] was used for the Google command task with a learning rate of 0.001. The retention ratios were randomly sampled and not trained in any of the low pass RNN models. Current literature uses task-specific initialization constraints help RNNs solve the addition and copying tasks better [35, 45]. Instead of that, we use a data-driven **curriculum learning protocol** in our experiments.

Temporal addition task The addition task [45] involves processing two parallel input data streams of equal length. The first stream comprises random numbers $\in (0, 1)$ and the second is full of zeros except at 2 time steps. At the end of the sequence, the network should output the sum of the two numbers in the first data stream corresponding to the time-steps when the second stream had non-zero entries. The baseline to beat is a mean square error (mse) of 0.1767, corresponding to a network that always generates 1. We first train the RNN cell on a short sequence and progressively increase the length. Each curriculum used 10,000 training and 1000 test samples. The results are shown in Figures 3, where each stage of the curriculum learning process is marked with bands of different colours. The width of the band indicates the number of epochs taken for convergence. The length of the task was incremented when the mse went below 0.001. With random initialization, the SimpleRNN cell failed to converge beyond sequence length 40, even with curriculum learning. We observe that both the lpRNN and LSTM cells benefit from the curriculum learning protocol. The lpRNN cell was able to transfer learning for sequences shorter than 150 steps. While, the benefits of curriculum learning appears to have reduced beyond that, the lpRNN cells were able to achieve better than 0.001 mse for sequences up to 642. While the performance of the lpRNN cell is at par or slightly inferior to other works in literature [39, 44, 45, 37], we achieved this result purely by random initialization. Another interesting outcome of this experiment was the effectiveness of a 2-unit LSTM cell in solving this task. It was able to add sequences much longer (we tested up to 100K) than any reported work. We made the task more complex by allowing the second stream to have up to 10 unmasked entries during training. The trained cell was tested with a data stream having more than 10 masked entries. The LSTM cell was successful in solving this problem a mse less than $1e-3$, indicating that it learnt a general add and accumulate operation. Figure 3c shows the evolution of the gating functions, internal state, and the state variables of an LSTM cell that was trained only on a fixed length sequence of 100 with mse less than 0.001. Contrast this against the stable dynamics of the network trained by curriculum learning in Figure 3d in a 100K sequence with mse less than $1e-3$ (Figure 3) indicating almost perfect long-term memory and addition. To our knowledge, this kind of generalized learning by an LSTM cell has not been shown before.

Temporal copying task We train the RNN cells on a varying length copying task as defined in [48] instead of the original definition [39, 44]. The network receives a sequence of up to S symbols (in the original definition, S is fixed) drawn from an alphabet of size K . At the end of S symbols, a sequence of T blank symbols ending with a trigger symbol is passed. The trigger symbol indicates that the network should reproduce the first S symbols in the same order. We first train the network on a short sequence ($T=3$) and gradually increase it ($T \leq 200$). The sequence length is incremented when the categorical accuracy is better than 99%. The SimpleRNN cell failed at this task even for $T=30$ with categorical accuracy dropping to 84% when it predicted only $S + T$ blank symbols. The lpRNN cell was able to achieve 99% accuracy for up to 120 time steps. After that, it generates T blank entries accurately but the accuracy of the last S symbols drops (For $T=200$, it was 96%). However, the LSTM cell achieves more than 99.5+% accuracy for all tested sequence lengths, highlighting the advantage of curriculum learning. This is a big improvement over reported results [44, 48, 49] where an LSTM cell does very poorly in this task. We too faced stability issues when training an LSTM cell for sequences longer than 30, even if it eventually converged by using smaller learning rates and gradient norm scaling. This makes a good test case to validate the temporal regularization property of the lpLSTM cell. In our tests, the lpLSTM cell converged without instability with categorical accuracy higher than 99.5% for all tested values of $T (\in [3, 500])$. It also to generalized larger values of S than the other cells (≤ 25). The lpLSTM cell exhibited a gradual degradation in performance for larger values of S . We stop our simulations when the categorical accuracy fell below 96%. These results are summarized in Figure 4.

Penn Treebank (PTB) [50] character model We studied temporal regularization in a network trained on the PTB dataset by replacing the LSTM cells by its low pass variants. We choose a model with 19M parameters and trained all variants using the same settings as described in [46] for 25 epochs. We note that both lpLSTM cells converge to a better score on the training set and a marginally poorer score on the train/validation set (refer Table 1). The lpLSTM cell with relu activation also converges unlike the plain relu LSTM cell validating our claim on temporal regularization.

Google commands dataset The Google commands dataset [24] comprises 36 classes of short length spoken commands such as “left”, “up”, “go”, etc. The dataset was created for hardware and algorithm developers to evaluate their low footprint neural network models in limited dictionary

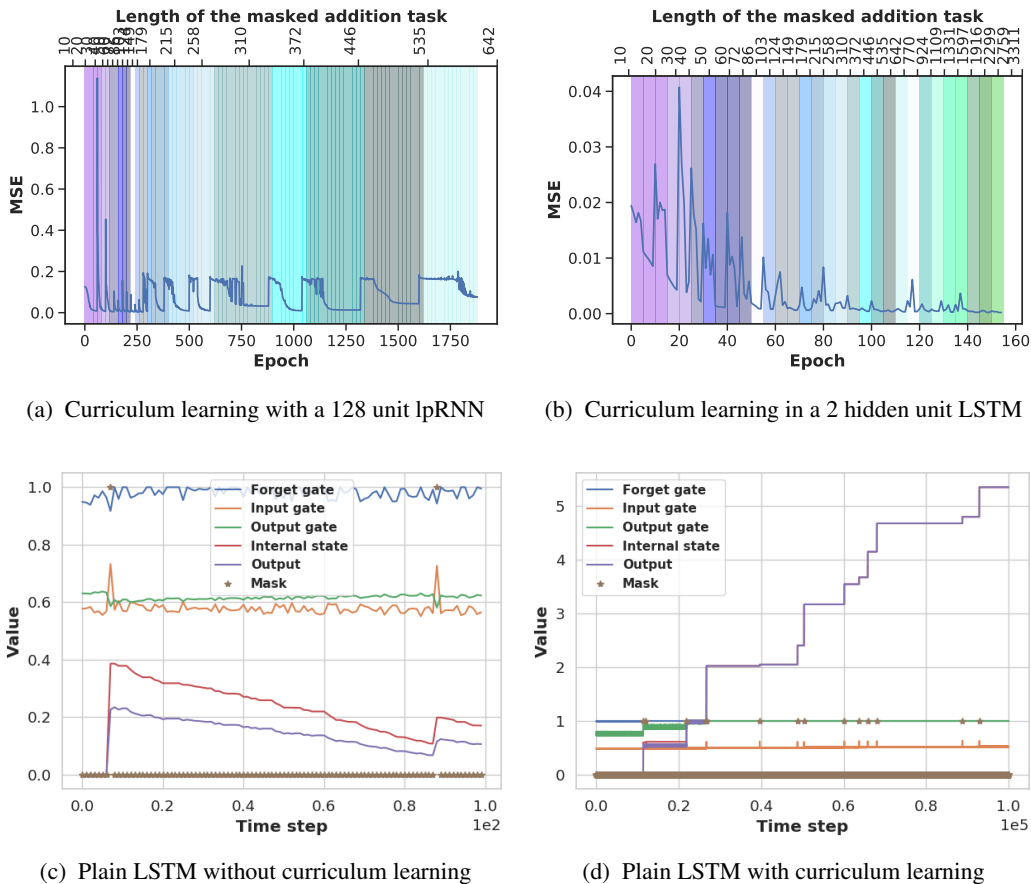


Figure 3: Curriculum learning on the masked addition task. LSTM cell trained without curriculum learning results in unstable state variables (c). When trained with curriculum learning it looks much more stable (d). Stars in (c) and (d) indicate value of the add mask.

Table 1: Impact of temporal regularization on the Penn Treebank model.

	Activation	Train perplexity	Validation Perplexity	Test Perplexity
LSTM	relu	approx. 641	approx. 641	Fails to converge
	tanh	46.0948	83.9807	80.0873
lpLSTM	tanh	41.0545	84.6127	81.7519
	relu	43.0602	84.1484	80.6946

speech recognition tasks. The reference neuromorphic platform proposed in Figure 2 is a natural fit for this task. Most neuromorphic platforms are also highly resource-constrained, due to power and size restrictions and can only implement small network models. To benchmark the performance of the lpRNN cell, we compare it against SimpleRNN, LSTM, and lpLSTM networks, all with roughly 80K trainable parameters. All the networks received Mel-spectrogram as inputs. This was connected to 2 fully-connected dense layers with 128 and 32 units, followed by two stages of RNN units (64 units in LSTM and lpLSTM, 128 units in lpRNN and SimpleRNN case). The RNN outputs were then processed by 2 fully-connected stages, topped by a softmax readout. Note that dense layers were used in these models as they are compatible with the reference SNN accelerator shown in Figure 2. The performance of the networks in all the 3 cases is illustrated in Figure 5. Both the LSTM and lpLSTM networks fit the training set with 99% categorical accuracy and the lpRNN cell came very close at 97%. We also saw a 2% gap in the validation set performance between the lpRNN and LSTM cells.

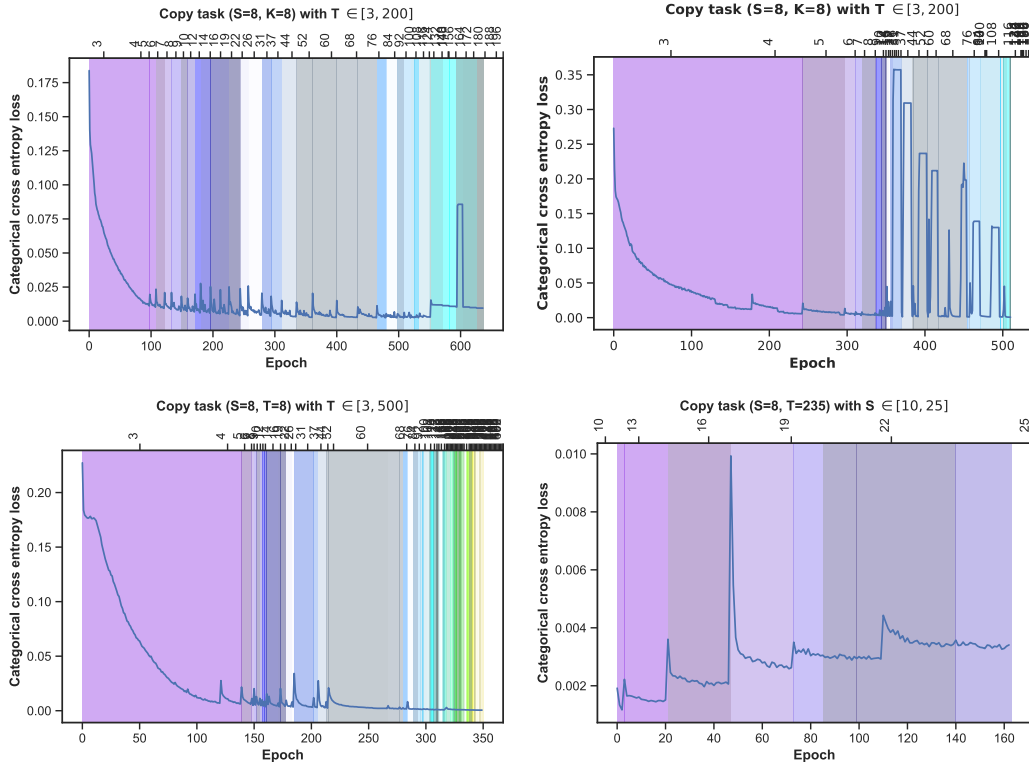


Figure 4: Curriculum learning on the variable length copying task for a 256 unit lpRNN (top left) and a 128 unit LSTM cell (top right) and a 128 unit lpLSTM cell (bottom left and right).

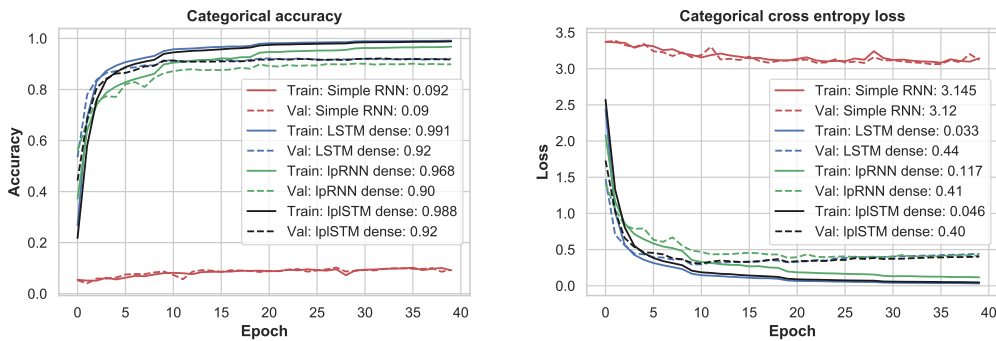


Figure 5: Performance on Google commands detection task: Accuracy (Left) and loss (Right).

8 Conclusion and outlook

This paper presents a low pass filtering enhancement to RNNs with the motivation to train an RNN with the back-propagation algorithm and deploy as a spiking neural network with no loss of accuracy. Interestingly, we also observe that low pass filtering has a temporal regularization effect that stabilizes learning and improves RNN performance remarkably. We formulate a general extension to ANN-RNN cells on this basis. We see that the low pass RNN models outperform their unfiltered counterparts in a range of synthetic and real-world datasets. The low pass enhancement will be instrumental in our future work on ultra-low power neuromorphic RNN accelerators for temporal processing tasks such as spoken command detection.

References

- [1] John Von Neumann. First draft of a report on the edvac. *IEEE Annals of the History of Computing*, 15(4):27–75, 1993.
- [2] Tom Shanley. *x86 Instruction Set Architecture*. MindShare press, 2010.
- [3] Stephen Bo Furber and Stephen B Furber. *ARM system Architecture*. Addison-Wesley Menlo Park, 1996.
- [4] Robert R Schaller. Moore’s law: past, present and future. *IEEE spectrum*, 34(6):52–59, 1997.
- [5] M Mitchell Waldrop. The chips are down for moore’s law. *Nature News*, 530(7589):144, 2016.
- [6] Alessandro Aimar, Hesham Mostafa, Enrico Calabrese, Antonio Rios-Navarro, Ricardo Tapiador-Morales, Iulia-Alexandra Lungu, Moritz B Milde, Federico Corradi, Alejandro Linares-Barranco, Shih-Chii Liu, et al. Nullhop: A flexible convolutional neural network accelerator based on sparse representations of feature maps. *IEEE transactions on neural networks and learning systems*, 2018.
- [7] Lukas Cavigelli and Luca Benini. Origami: A 803-gop/s/w convolutional network accelerator. *IEEE Transactions on Circuits and Systems for Video Technology*, 27(11):2461–2475, 2016.
- [8] Yu-Hsin Chen, Tushar Krishna, Joel S Emer, and Vivienne Sze. Eyeriss: An energy-efficient reconfigurable accelerator for deep convolutional neural networks. *IEEE Journal of Solid-State Circuits*, 52(1):127–138, 2016.
- [9] Charlotte Frenkel, Martin Lefebvre, Jean-Didier Legat, and David Bol. A 0.086-mm² 12.7-pj/sop 64k-synapse 256-neuron online-learning digital spiking neuromorphic processor in 28-nm cmos. *IEEE transactions on biomedical circuits and systems*, 13(1):145–158, 2019.
- [10] Mike Davies, Narayan Srinivasa, Tsung-Han Lin, Gautham Chinya, Yongqiang Cao, Sri Harsha Choday, Georgios Dimou, Prasad Joshi, Nabil Imam, Shweta Jain, et al. Loihi: A neuromorphic manycore processor with on-chip learning. *IEEE Micro*, 38(1):82–99, 2018.
- [11] S. Moradi, N. Qiao, F. Stefanini, and G. Indiveri. A scalable multicore architecture with heterogeneous memory structures for dynamic neuromorphic asynchronous processors (DYNAPs). *Biomedical Circuits and Systems, IEEE Transactions on*, 12(1):106–122, Feb. 2018.
- [12] Filipp Akopyan, Jun Sawada, Andrew Cassidy, Rodrigo Alvarez-Icaza, John Arthur, Paul Merolla, Nabil Imam, Yutaka Nakamura, Pallab Datta, Gi-Joon Nam, et al. Truenorth: Design and tool flow of a 65 mw 1 million neuron programmable neurosynaptic chip. *IEEE Transactions on Computer-Aided Design of Integrated Circuits and Systems*, 34(10):1537–1557, 2015.
- [13] Ning Qiao, Hesham Mostafa, Federico Corradi, Marc Osswald, Fabio Stefanini, Dora Sumislawska, and Giacomo Indiveri. A reconfigurable on-line learning spiking neuromorphic processor comprising 256 neurons and 128k synapses. *Frontiers in neuroscience*, 9:141, 2015.
- [14] Alexander Neckar, Sam Fok, Ben V Benjamin, Terrence C Stewart, Nick N Oza, Aaron R Voelker, Chris Eliasmith, Rajit Manohar, and Kwabena Boahen. Braindrop: A mixed-signal neuromorphic architecture with a dynamical systems-based programming model. *Proceedings of the IEEE*, 107(1):144–164, 2019.
- [15] Melika Payvand, Manu V Nair, Lorenz K Müller, and Giacomo Indiveri. A neuromorphic systems approach to in-memory computing with non-ideal memristive devices: From mitigation to exploitation. *Faraday Discussions*, 213:487–510, 2019.
- [16] Ping Chi, Shuangchen Li, Cong Xu, Tao Zhang, Jishen Zhao, Yongpan Liu, Yu Wang, and Yuan Xie. Prime: A novel processing-in-memory architecture for neural network computation in rram-based main memory. In *ACM SIGARCH Computer Architecture News*, volume 44, pages 27–39. IEEE Press, 2016.

- [17] Junwhan Ahn, Sungjoo Yoo, Onur Mutlu, and Kiyoun Choi. Pim-enabled instructions: a low-overhead, locality-aware processing-in-memory architecture. In *2015 ACM/IEEE 42nd Annual International Symposium on Computer Architecture (ISCA)*, pages 336–348. IEEE, 2015.
- [18] Peter U Diehl, Daniel Neil, Jonathan Binas, Matthew Cook, Shih-Chii Liu, and Michael Pfeiffer. Fast-classifying, high-accuracy spiking deep networks through weight and threshold balancing. In *2015 International Joint Conference on Neural Networks (IJCNN)*, pages 1–8. IEEE, 2015.
- [19] Bodo Rueckauer, Iulia-Alexandra Lungu, Yuhuang Hu, Michael Pfeiffer, and Shih-Chii Liu. Conversion of continuous-valued deep networks to efficient event-driven networks for image classification. *Frontiers in neuroscience*, 11:682, 2017.
- [20] Sander M Bohte. Efficient spike-coding with multiplicative adaptation in a spike response model. In *Advances in Neural Information Processing Systems*, pages 1835–1843, 2012.
- [21] Hesham Mostafa. Supervised learning based on temporal coding in spiking neural networks. *IEEE transactions on neural networks and learning systems*, 29(7):3227–3235, 2017.
- [22] M. V. Nair and G. Indiveri. An ultra-low power sigma-delta neuron circuit. In *2019 IEEE International Symposium on Circuits and Systems (ISCAS)*, pages 1–5, May 2019.
- [23] Yoshua Bengio, Jérôme Louradour, Ronan Collobert, and Jason Weston. Curriculum learning. In *Proceedings of the 26th annual international conference on machine learning*, pages 41–48. ACM, 2009.
- [24] Pete Warden. Speech commands: A dataset for limited-vocabulary speech recognition. *arXiv preprint arXiv:1804.03209*, 2018.
- [25] Romain Brette and Wulfram Gerstner. Adaptive exponential integrate-and-fire model as an effective description of neuronal activity. *Journal of neurophysiology*, 94(5):3637–3642, 2005.
- [26] Young C Yoon. Lif and simplified srm neurons encode signals into spikes via a form of asynchronous pulse sigma–delta modulation. *IEEE transactions on neural networks and learning systems*, 28(5):1192–1205, 2016.
- [27] Wulfram Gerstner and Werner M Kistler. *Spiking neuron models: Single neurons, populations, plasticity*. Cambridge university press, 2002.
- [28] Herbert Jaeger, Mantas Lukoševičius, Dan Popovici, and Udo Siewert. Optimization and applications of echo state networks with leaky-integrator neurons. *Neural networks*, 20(3):335–352, 2007.
- [29] Manu Nair. Github repo - <https://github.com/manuvm/sigma-delta-neural-networks>, February 2019.
- [30] Vincent Chan, Shih-Chii Liu, and Andr van Schaik. Aer ear: A matched silicon cochlea pair with address event representation interface. *IEEE Transactions on Circuits and Systems I: Regular Papers*, 54(1):48–59, 2007.
- [31] Rahul Sarpeshkar, Richard F Lyon, and Carver Mead. A low-power wide-dynamic-range analog vlsi cochlea. In *Neuromorphic systems engineering*, pages 49–103. Springer, 1998.
- [32] Tara Julia Hamilton, Craig Jin, Andre Van Schaik, and Jonathan Tapson. An active 2-d silicon cochlea. *IEEE Transactions on biomedical circuits and systems*, 2(1):30–43, 2008.
- [33] Saugata Ghose, Kevin Hsieh, Amirali Boroumand, Rachata Ausavarungnirun, and Onur Mutlu. Enabling the adoption of processing-in-memory: Challenges, mechanisms, future research directions. *arXiv preprint arXiv:1802.00320*, 2018.
- [34] Yiren Wang and Fei Tian. Recurrent residual learning for sequence classification. In *Proceedings of the 2016 Conference on Empirical Methods in Natural Language Processing*, pages 938–943, 2016.

- [35] Mikael Henaff, Arthur Szlam, and Yann LeCun. Recurrent orthogonal networks and long-memory tasks. *arXiv preprint arXiv:1602.06662*, 2016.
- [36] Shuai Li, Wanqing Li, Chris Cook, Ce Zhu, and Yanbo Gao. Independently recurrent neural network (indrnn): Building a longer and deeper rnn. In *Proceedings of the IEEE Conference on Computer Vision and Pattern Recognition*, pages 5457–5466, 2018.
- [37] Yuhuang Hu, Adrian Huber, Jithendar Anumula, and Shih-Chii Liu. Overcoming the vanishing gradient problem in plain recurrent networks. *arXiv preprint arXiv:1801.06105*, 2018.
- [38] Razvan Pascanu, Tomas Mikolov, and Yoshua Bengio. On the difficulty of training recurrent neural networks. In *International Conference on Machine Learning*, pages 1310–1318, 2013.
- [39] Sepp Hochreiter and Jürgen Schmidhuber. Long short-term memory. *Neural computation*, 9(8):1735–1780, 1997.
- [40] Felix A Gers, Jürgen Schmidhuber, and Fred Cummins. Learning to forget: Continual prediction with lstm. *Neural Computation*, 12(10):2451–2471, 2000.
- [41] Junyoung Chung, Caglar Gulcehre, KyungHyun Cho, and Yoshua Bengio. Empirical evaluation of gated recurrent neural networks on sequence modeling. *arXiv preprint arXiv:1412.3555*, 2014.
- [42] Daniel Neil, Michael Pfeiffer, and Shih-Chii Liu. Phased lstm: Accelerating recurrent network training for long or event-based sequences. In *Advances in neural information processing systems*, pages 3882–3890, 2016.
- [43] SHI Xingjian, Zhouong Chen, Hao Wang, Dit-Yan Yeung, Wai-Kin Wong, and Wang-chun Woo. Convolutional lstm network: A machine learning approach for precipitation nowcasting. In *Advances in neural information processing systems*, pages 802–810, 2015.
- [44] Martin Arjovsky, Amar Shah, and Yoshua Bengio. Unitary evolution recurrent neural networks. In *International Conference on Machine Learning*, pages 1120–1128, 2016.
- [45] Quoc V Le, Navdeep Jaitly, and Geoffrey E Hinton. A simple way to initialize recurrent networks of rectified linear units. *arXiv preprint arXiv:1504.00941*, 2015.
- [46] Yoon Kim, Yacine Jernite, David Sontag, and Alexander M Rush. Character-aware neural language models. In *Thirtieth AAAI Conference on Artificial Intelligence*, 2016.
- [47] Diederik P Kingma and Jimmy Ba. Adam: A method for stochastic optimization. *arXiv preprint arXiv:1412.6980*, 2014.
- [48] Alex Graves, Greg Wayne, and Ivo Danihelka. Neural turing machines. *arXiv preprint arXiv:1410.5401*, 2014.
- [49] Shaojie Bai, J Zico Kolter, and Vladlen Koltun. An empirical evaluation of generic convolutional and recurrent networks for sequence modeling. *arXiv preprint arXiv:1803.01271*, 2018.
- [50] Mitchell Marcus, Grace Kim, Mary Ann Marcinkiewicz, Robert MacIntyre, Ann Bies, Mark Ferguson, Karen Katz, and Britta Schasberger. The penn treebank: annotating predicate argument structure. In *Proceedings of the workshop on Human Language Technology*, pages 114–119. Association for Computational Linguistics, 1994.